Res Chem Intermed (2014) 40:1233–1247
DOI 10.1007/s11164-013-1035-1

Morphology of polyaniline nanofibers synthesized under different conditions

Fereshteh Rezaei · Nahid Pirhady Tavandashti · Ali Reza Zahedi

Received: 13 November 2012 / Accepted: 8 January 2013 / Published online: 5 February 2013

Abstract Polyaniline nanofibers are readily synthesized by bulk polymerization; ammonium per sulphate (APS) is used as oxidizing agent and hydrochloric acid as dopant without any hard or soft templates. A detailed study was conducted on the effect of a variety of synthetic conditions on the size and morphology of the polyaniline nanostructure. These conditions include the concentration of dopant, and the APS-to-aniline and acid-to-aniline molar ratios. The morphology of the nanofibers was confirmed by SEM and TEM. XRD and FT-IR and UV–visible spectroscopy were used for structural characterization of nanofibers. The results showed that not only the microstructure of the polyaniline product, but also other characteristics, for example conductivity, crystallinity, and, more importantly, the efficiency of the process are strongly affected by the synthetic conditions.

Keywords Polyaniline · Nanofiber · Morphology · APS · Dopant

Introduction

Since 1980, many studies have been performed on conducting polymers, because of their attractive electrical and optical properties resulting from their conjugated π-electron systems [1, 2]. However, polyaniline has unique advantages among other conducting polymers, for example easy synthesis, low cost monomer, environmental stability, and facile acid/base doping/dedoping chemistry [2]. Polyaniline nanostructures have been used for a variety of applications in different fields, for example corrosion inhibitors [3], anticorrosion coatings [4], electrodes, capacitors [5], rechargeable batteries [6] chemical sensors [7], semiconductors, and electromagnetic shielding devices [8].

F. Rezaei (✉) · N. P. Tavandashti · A. R. Zahedi
Coating Research Center, Research Institute of Petroleum Industry, Tehran, Iran
e-mail: rezaeif@gmail.com; rezaeif@ripi.ir

Nanostructured polyaniline (nano-rods, wires, and fibers) offers the possibility of enhanced performance whenever a high interfacial area between polyaniline and its environment is important [9]. Different methods have been used for synthesis of polyaniline nanofibers, including template guided polymerization using zeolites as hard templates or surfactants, micelles, liquid crystals, and polyacids as soft templates [9–11]. Because all these methods depend on use of either a template or a specific complex chemical reagent, after-synthesis treatments are necessary to remove them from the products to recover pure nanostructured polyaniline. Therefore developing syntheses that do not rely on templates, structural directing molecules, or specific dopants are of great importance. Different templateless polymerization, for example interfacial polymerization [12], oligomer-assisted polymerization [13], and seeding polymerization [14] have been reported in the literature. However, some synthetic conditions including monomer concentration, solution pH, types of dopant and oxidizing agent, mechanical stirring, reaction time and temperature are important in all of the polymerization methods. These conditions can affect the molecular weight, morphology, and molecular structure.

Conventional synthesis of polyaniline usually involves chemical oxidative polymerization of aniline, in solution, in the presence of a suitable oxidant, for example ammonium peroxydisulfate (APS) [9]. However, the mechanism of formation of polyaniline nanofibers is associated with the linear nature of polyaniline chains [9]; nanofibers seem to have the intrinsic morphology of polyaniline even when conventional synthesis is used. Therefore, it is possible to produce PAni nanofibers without using hard or soft templates.

It is suggested that particle morphology can be correlated with the mode of nucleation of polyaniline—homogeneous nucleation of polyaniline results in nanofibers whereas heterogeneous nucleation leads to granular particulates [15]. However, both homogeneous and heterogeneous nucleation occurs in the conventional synthesis of polyaniline [15], resulting in irregularly shaped granular particles. Therefore, to produce polyaniline nanofibers, heterogeneous nucleation should be suppressed throughout the polymerization process, which will enable polyaniline nanofibers to form continuously via homogeneous nucleation. For this purpose, it is recommended polyaniline molecules are produced rapidly; it is then more likely these embryonic nuclei will evolve to cause homogeneous nucleation because it takes time to diffuse to heterosites [2, 15, 16].

The purpose of this study was to develop a templateless method for production of nano fibrous polyaniline based on a simple bulk polymerization process. The nanofibers were readily obtained by rapid mixing of aniline with oxidant in an aqueous acidic solution at 40 °C then allowing the polymerization to proceed to completion in the absence of mechanical agitation. The effect of the concentrations of aniline monomer, APS oxidant, and HCl dopant on the microstructure and morphology of PAni were investigated. To study the effect of these by use of the smallest number of test runs, experiments were designed using interrelated conditions, including acid-to-aniline and APS-to-aniline molar ratios and the molarity of the acid.

Experimental

Materials

The precursors used for synthesis of PAni were aniline purchased from Sigma–Aldrich and ammonium persulfate (APS) and hydrochloric acid purchased from Merck. All reagents were used without further purification.

Synthesis of PAni nanofibers

HCl solution of different molarity (0.1, 0.5 and 1 M) was prepared. The solution was divided into two parts labeled (a) and (b). The temperature of the solution was adjusted to 40 °C by use of a water bath. Aniline monomer was introduced into part (a) of acidic solution and APS oxidant was similarly dissolved in part (b). The two solutions were mixed rapidly and the temperature was kept at 40 °C for 3.5 h. The solution was not stirred or agitated during polymerization process. The other synthetic conditions were acid-to-aniline monomer molar ratios (A/M) of 10, 100, and 652, and APS-to-aniline molar ratios (APS/aniline) of 0.25, 0.5, and 1.

The dark green polyaniline product was washed several times and centrifuged to collect the material, which was then introduced into a special tubular dialysis membrane with molecular weight cut-off (MWCO) of 12,000–14,000. Dialysis with deionized water was performed for 24 h, when the pH of the system had reached 5–7.

Characterization

The structure of the samples was observed by scanning electron microscopy (SEM; TeScan model Vegall XMU). Samples for transmission electron microscopy (TEM; Zeiss-EM900) were prepared on copper grids. X-ray diffraction (XRD) patterns were obtained by use of an X-ray diffractometer (Philips model pw1840) with Ni-filtered Cu Kα radiation. UV–visible absorbance spectra were studied by use of a Perkin–Elmer Lambda 9 spectrometer; the polyaniline was dissolved in *N*-methyl-2-pyrrolidinone (NMP) solvent. Fourier-transform infrared (FT-IR) was used to characterize molecular structures of PAni nanofibers. FT-IR spectra of the composites in KBr pellets were recorded in transmission mode on an Equinox 55 FT-IR spectrometer. The spectra were collected from 500 to 4,000 cm^{-1}. The conductivity of the nanofiber products was measured at room temperature by the use of a Philips PM 2519 multimeter. Electrical conductivity measurements were performed on a disk 13 mm in diameter and 0.3 mm thick which was prepared under 10 MPa pressure. Copper paste was used to eliminate the connection resistance.

Results and discussion

Chemical oxidative polymerization of aniline is one of the traditional methods of synthesis of polyaniline in bulk quantities [16, 17]. Observations have indicated that nanofibers are definitely formed in the conventional polymerization process

[18–20]; however, renucleation of more polyaniline on their surface rapidly produces irregularly shaped agglomerates as the reaction proceeds. Pure polyaniline fibers can be obtained by preventing the heterogeneous nucleation which leads to subsequent overgrowth of polyaniline on the nanofibers [18–20]. Faster polymerization seems to favor homogeneous nucleation, because a higher transient concentration of polyaniline molecules facilitates formation of more homogeneous nuclei at the beginning of precipitation. Moreover, if polyaniline molecules are produced rapidly it is more likely that these embryonic nuclei will evolve to create homogeneous nuclei, because it takes time to diffuse to heterosites [15]. Hence, rapid mixing of the two reactant solutions and performing the reaction at higher temperatures are beneficial for generating nanofibers, because they enable polyaniline molecules to form quickly [2].

Taking all these experimental factors into account, high-quality polyaniline nanofibers were easily achieved in this work by rapidly mixing aniline with APS oxidant in an aqueous HCl at 40 °C without any mechanical agitation. Figure 1 shows typical SEM and TEM images of the as-synthesized polyaniline nanofibers; these reveal that the PAni product is composed of a large quantity of high-quality nanofibers. It is observed that these polyaniline nanofibers have diameters in the range 40–70 nm and their length is approximately one to several microns.

To find the optimum conditions for synthesis of polyaniline nanofibers by use of this method, the effects of the concentrations of aniline monomer, APS oxidant, and HCl dopant were investigated. The appropriate conditions for obtaining PAni most efficiently were also examined.

To study the effect of molar ratio of APS to aniline, samples were prepared using hydrochloric acid with different APS-to-aniline molar ratios (i.e. 0.125, 0.25, 0.5, or 1). The other conditions were kept constant for all samples; i.e. the molarity of acid used for synthesis of the samples shown in Figs. 2 and 3 was 0.1 and 0.5 M, respectively, and acid-to-aniline molar ratios for these samples were 10 and 100, respectively.

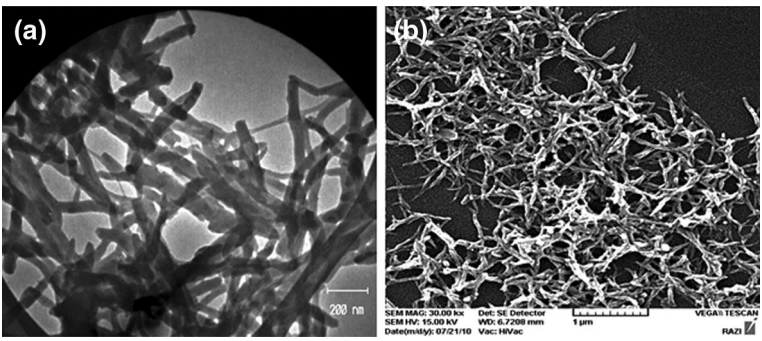

Fig. 1 TEM (**a**) and SEM (**b**) images of the as-synthesized polyaniline nanofibers

The SEM micrographs of PAni samples shown in Fig. 2a–d reveal that the lower the APS-to-aniline molar ratio, the finer the structure of the products, with smaller average diameter of the fibers. Moreover, when the molar ratio of APS to aniline is increased, nucleation of knots on the surface of the fibers is distinctly evident, indicating that increasing the concentration of APS can induce heterogeneous nucleation on the surfaces of polyaniline nanofibers to form nanoparticles [21].

The SEM micrographs of the PAni samples synthesized using 0.5 M acid and an acid-to-aniline molar ratio of 100, shown in Fig. 3a–c, also illustrates that the average diameter of the polyaniline nanofibers increases as the concentration of APS increases. When lower concentrations of APS are used the PAni nanofibers are more likely to have a longer and less branched structure. It has been reported that higher oligomer concentration favors homogeneous nucleation, which reduces secondary nucleation sites on already existing nanofibers [22, 23]. However, excessive APS may reduce the rate of polymerization [1] and, consequently, may reduce the concentration of oligomers, which may induce heterogeneous nucleation to form small white spots on the surfaces of nanofibers.

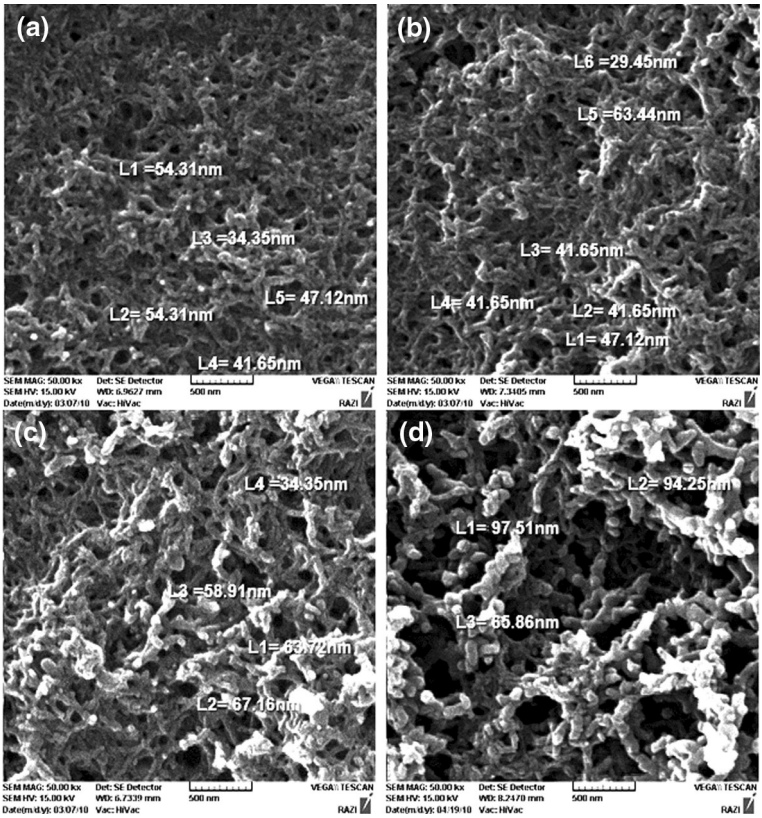

Fig. 2 SEM images of the PAni produced using: 0.1 M HCl, acid/aniline molar ratio = 10 and APS/aniline molar ratio = 0.125 (**a**), 0.25 (**b**), 0.5 (**c**), and 1 (**d**)

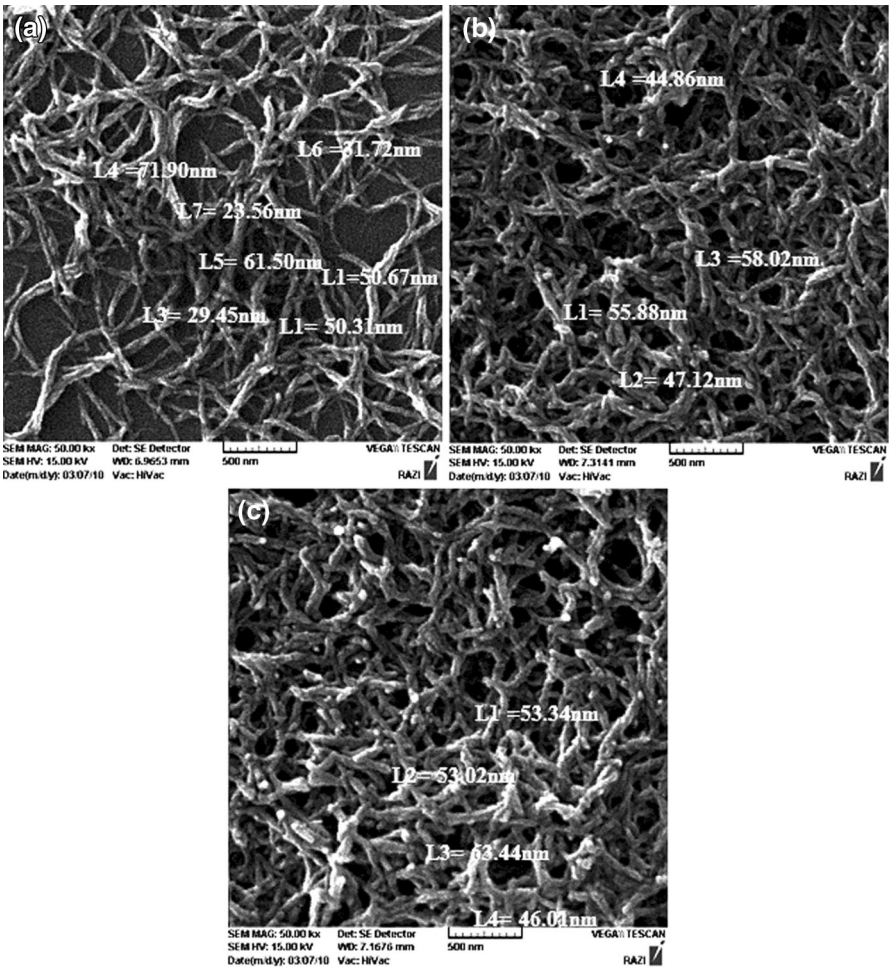

Fig. 3 SEM images of the PAni produced using: 0.5 M HCl, acid/aniline molar ratio = 100 and APS/aniline molar ratio = 0.125 (**a**), 0.25 (**b**), and 0.5 (**c**)

It should be mentioned that the PAni nanofibers in Fig. 3 synthesized by use of 0.5 M HCl and an acid-to-aniline molar ratio of 100 are longer than the nanofibers of Fig. 2 synthesized by use of 0.1 M HCl and an acid-to-aniline molar ratio of 10 and corresponding APS-to-aniline molar ratios. This implies that the molarity of the acid and the acid-to-aniline molar ratio are also important conditions affecting the structure and morphology of the polyaniline samples.

Figures 4 and 5 show the effect of the molarity of the acid used to synthesize polyaniline nanofibers. The figures show samples prepared using different HCl molarities (0.1, 0.5, or 1 M), with other conditions kept constant. Almost the same trend is observed in both figures despite synthesis being performed with two different aniline concentrations. In Fig. 4a, for which 0.5 M HCl was used, fibers with a finer structure and average diameter of approximately 50 nm were formed.

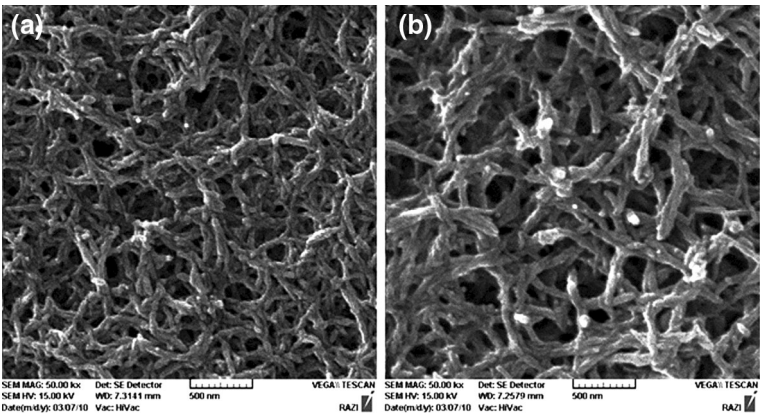

Fig. 4 SEM micrographs of the PAni produced using: acid/aniline molar ratio = 100, APS/aniline molar ratio = 0.25 and molarity of acid = 0.5 M (**a**) and 1 M (**b**)

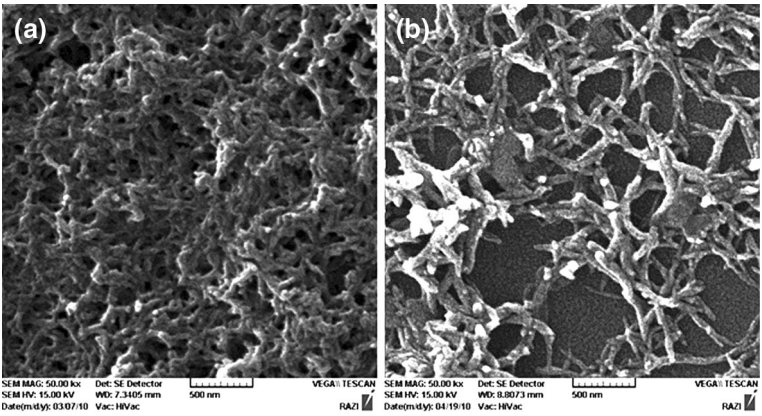

Fig. 5 SEM micrographs of the PAni produced using: acid/aniline molar ratio = 10, APS/aniline molar ratio = 0.25 and molarity of acid = 0.1 M (**a**) and 0.5 M (**b**)

When the molarity of the acid was increased to 1 M (Fig. 4b) an increase in the average diameter is observed (approx. 70 nm). Furthermore, in Fig. 5a, for which 0.1 M HCl was used, fibers with an average diameter of approximately 45 nm were formed, and when the molarity of the acid was increased to 0.5 M (Fig. 5b) the average diameter increased to approximately 65 nm. Moreover, Fig. 4a, b show the average length of the fibers increased from 0.5–1 μm to 1–2 μm on increasing the molarity of the acid from 0.5 to 1 M whereas Fig. 5a, b shows the average length of the fibers increased from <0.5 to 0.5–1.5 μm on increasing the molarity of the acid from 0.1 to 0.5 M.

It is also worth mentioning that the polyaniline nanofibers shown in Figs. 4 and 5 have smoother surfaces when lower concentrations of HCl were used for synthesis. By increasing the acid concentration the roughness of the surfaces of the nanofibers is increased. This may be because of enhancement of heterogeneous nucleation at

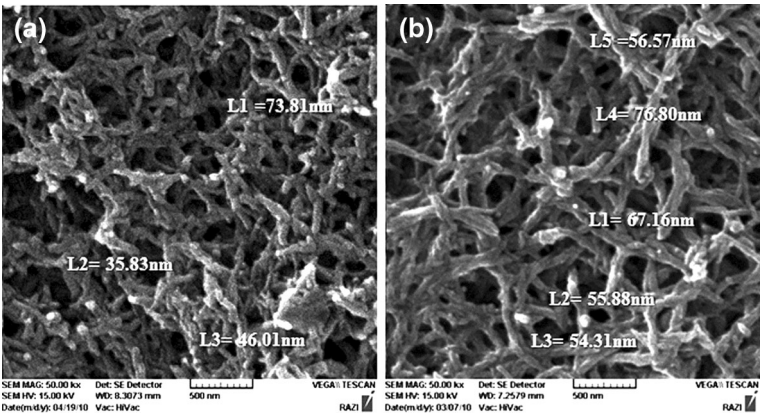

Fig. 6 SEM micrographs of the PAni produced using: 1 M HCl, APS/aniline molar ratio = 0.25 and acid/aniline molar ratio = 10 (**a**) and 100 (**b**)

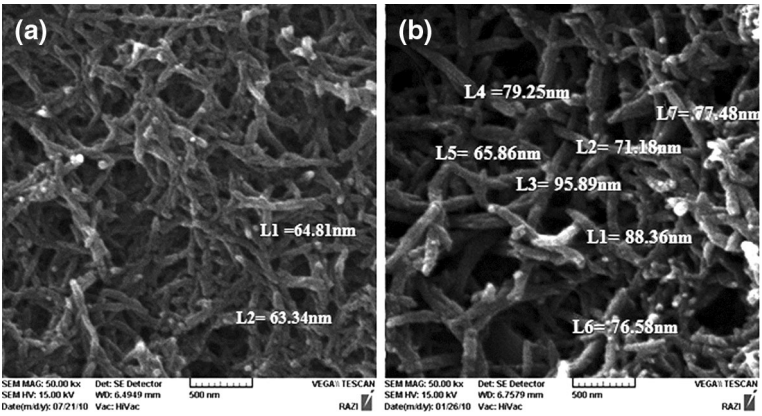

Fig. 7 SEM micrographs of the PAni produced using: 1 M HCl, APS/aniline molar ratio = 0.5 and acid/aniline molar ratio = 100 (**a**) and 652 (**b**)

higher acid concentrations, which induces active sites on the surfaces of polyaniline nanofibers [1].

To study the effect of the molar ratio of acid to aniline, samples were prepared by use of hydrochloric acid with different acid-to-aniline molar ratios (i.e. 10, 100, or 652). The other conditions were kept constant for all samples (i.e. acid concentration 1 M and APS-to-aniline molar ratio 0.25 or 0.5). Comparison of the microstructure of the PAni samples shown in Fig. 6a and b reveals that, for otherwise identical synthetic conditions, when the acid-to-aniline molar ratio was increased from 10 to 100 the diameter of the fibers increased from 30–60 nm to 55–80 nm. The same trend was observed when the microstructure of the PAni samples shown in Fig. 7 (samples produced using acid-to-aniline molar ratios of 10 or 652) was compared. On increasing acid-to-aniline molar ratio, the diameter of the polyaniline nanofibers increased from 45–65 nm (Fig. 7a) to 70–100 nm (Fig. 7b).

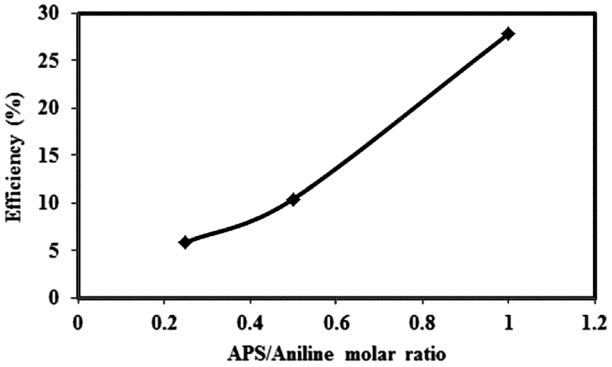

Fig. 8 The effect of APS/Aniline molar ratio on the efficiency of the process

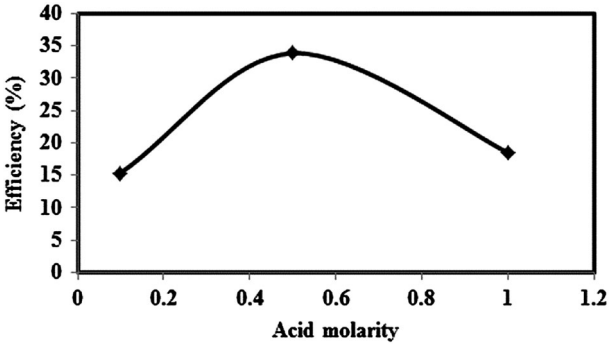

Fig. 9 The effect of molarity of Acid on the efficiency of the process

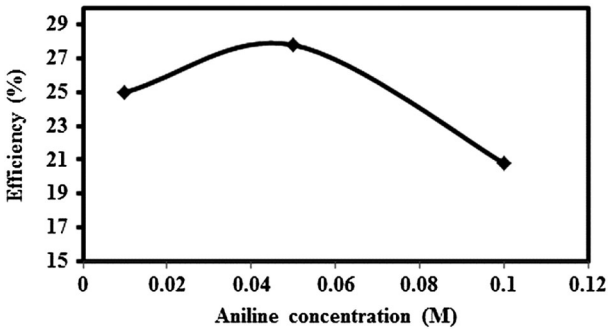

Fig. 10 The effect of aniline concentration on the efficiency of the process

These results indicate that acid-to-aniline molar ratio is very important in determining the diameter of the fibers. It has been reported that fiber formation during the oxidative chemical polymerization of aniline in an acidic medium involves a reactive intermediate species rearranged from protonated aniline [24].

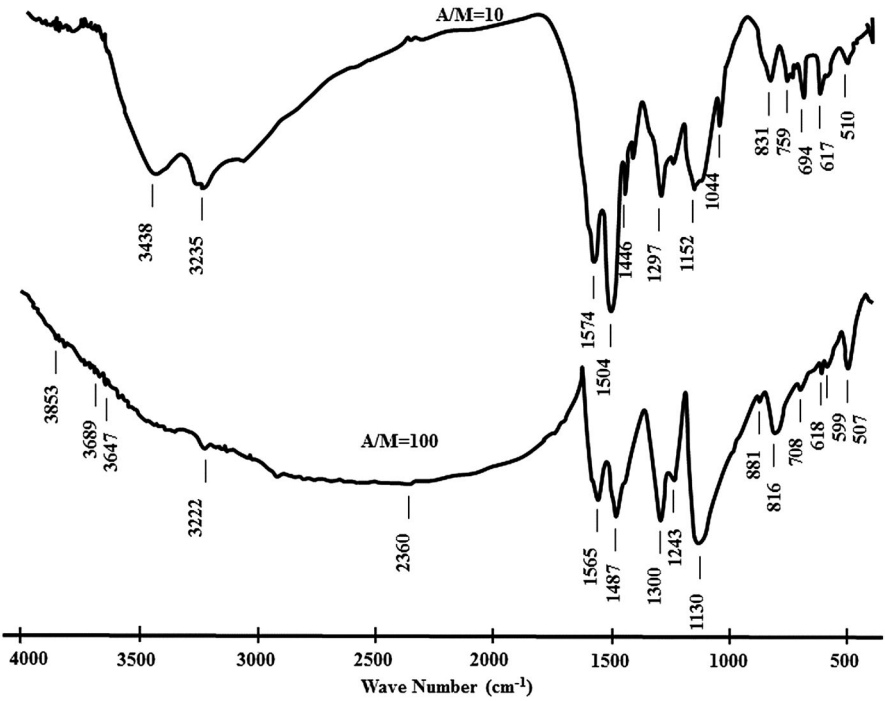

Fig. 11 The FTIR spectra of the samples prepared using acid/aniline = 10 and 100

When higher acid-to-aniline molar ratios are used the concentration of protonated aniline will increase, because of the higher concentration of H^+. The greater concentration of protonated aniline may result in the formation of nanofibers with larger diameters.

The effect of the synthetic conditions on the efficiency (%) of the process was also investigated by use of the equation:

$$\text{Efficiency } (\%) = \text{Weight of polymer (g)} / \text{aniline content (g)} \times 100 \quad (1)$$

Figures 8, 9, and 10 illustrate the effect of APS-to-aniline molar ratio, acid molarity, and aniline concentration, respectively, on efficiency. It is observed that when the APS-to-aniline molar ratio increases the efficiency obviously rises, indicating that APS-to-aniline molar ratio not only affects the morphology of the PAni product but also has an important effect on the efficiency of the process. However, the molarities of the acid and aniline do not seem to have significant effects on the efficiency of the process, despite having substantial effects on the morphology and structure of the polyaniline product.

The oxidation state and degree of protonation of conducting polymers can be evaluated FT-IR [25]. The FT-IR spectra of samples prepared by use of acid-to-aniline ratios of 10 and 100 are illustrated in Fig. 11. The vibration modes related to different characteristic peaks extracted from Fig. 11 are listed in Table 1. Results from some other work are also shown in Table 1 for comparison. Although the

Table 1 The vibration modes related to different characteristic peaks of polyaniline samples

Vibration mode	Measured data (cm^{-1})		Literature data (cm^{-1})		
	Acid/aniline = 10	Acid/aniline = 100	Nanofiber PAni-HCl [38]	Nanorod PAni-HCl [42]	Undoped PAni [42]
–C=C stretch vibration benzenoid ring	1,574	1,565	1,559	1,581	1,595
–C=C stretch vibration quinoid ring	1,504	1,487	1,480	1,494	1,501
C–N stretch	1,297	1,300	1,296	1,304	1,306
Protonated C–N group	1,241	1,243	1,242		
C–H in-plane bend	1,152	1,130	1,130	1,112	1,166
C–H out of plane	831	816	820	802	832

synthetic conditions were different in the different work, the characteristics of the polyaniline products are almost comparable. Considering Fig. 11 and Table 1 the results can be listed as follows:

- It has been reported [26] that the conductivity of polyaniline can be estimated from the ratio Q/B, where Q and B are the areas of peaks arising from the C=N bonds of quinoid units and C–N benzenoid units, respectively, in IR spectra. The degree of oxidation of polyaniline increases with increasing Q/B ratio and, hence, the number of quinoid rings in the molecular structure of the conducting polymer also increases. Visual comparison of the FT-IR spectra of both samples shows the Q/B ratio for the sample with acid/aniline = 100 is higher than that for the sample with acid/aniline = 10. Hence, with increasing the acid-to-aniline molar ratio the oxidation level of the polyaniline product is increased.
- As shown in Table 1, the characteristic vibrational bands of the sample with the lower acid-to-aniline molar ratio at 1574, 1504, 1297, 1152, and 831 cm^{-1} are shifted to 1565, 1487, 1300, 1130, and 820 cm^{-1} for the sample with higher acid/aniline ratio. It has been suggested that the increase of effective conjugation length can induce shifting of the characteristic vibrational bands of polymer backbone [27]. It also shows that the degree of doping decreases with decreasing acid concentration.
- A single peak occurs at 1,243 and 1,241 cm^{-1} in the spectra of samples with acid-to-aniline molar ratio of 100 and 10, respectively. This characteristic band is assigned to the C–N–C stretching vibration mode in the polaron structure [28].
- Two peaks at 1,446 and 1,044 cm^{-1} in the FT-IR spectrum of the sample with the lower acid-to-aniline molar ratio are assigned to benzene ring and C–H in-plane bending, respectively, of the 1,4 ring [29]. Both were absent from the FT-IR spectrum of the polymer with the higher acid-to-aniline molar ratio and thus the higher oxidation level.
- In the sample with the acid-to-aniline ratio of 100, the long absorption tail above 2,000 cm^{-1}, which masks the NH stretching vibration in the 3,100–3,500 cm^{-1} region, and appearance of the intense peak at 1,130 cm^{-1} have been associated

with high electrical conductivity and high degree of electron delocalization in PAni [30, 31].

The oxidation and reduction states of polyaniline during the doping process can be determined from the UV–visible absorption spectra of PAni/NMP solution [29]. Three characteristic bands in the wavelength ranges 250–320, 320–450, and 450–750 nm are usually observed in the UV–visible spectra of polyaniline. The first wavelength range is related to excitation of nitrogen in benzenoid rings (π–π* transition); the second and third are a result of polaron–bipolaron transitions in the emeraldine salt [32].

The UV–visible spectra of the three samples synthesized with the same acid-to-aniline molar ratio but with different molar concentrations of acid (0.1, 0.5, and 1 M) are presented in Fig. 12. The characteristic absorption peaks are observed at 344 and 625 nm for the sample prepared using an acid concentration of 1 M and at 333 and 628 nm for the sample prepared using an acid concentration of 0.5 M, because of the polaron–bipolaron equilibrium in the polymer structure, showing that the samples are in the emeraldine salt form [33, 34]. There is little difference between the UV–visible spectra of the two polyaniline samples synthesized using acid concentrations of 1 and 0.5 M. However, it is reported that the polarity of polyaniline may decrease in the presence of NMP as solvent. In fact, reduction of polyaniline occurs because of hydrogen bond formation between the C=O group in NMP and the NH segment of the polymer chain [35–37].

The characteristic absorption peaks observed at 254 and 357 nm for the sample prepared using an acid concentration of 0.1 M are assigned to a π transition in the benzenoid units and polaron–bipolaron transitions, respectively. However, no absorption peak is observed in the long wavelength range for the sample prepared using 0.1 M acid. This is because of the decrease in the polarity of the product as a result of the lower acid concentration used during synthesis.

The effect of dopant concentration on the conductivity of the polyaniline was also investigated. The conductivity of products prepared with acid concentrations of 1, 0.5 and 0.1 M was measured to be 116.83, 26.52, and 1.19 S cm^{-1}, respectively. These results show that with increasing dopant concentration, the conductivity and polarity of polyaniline increases.

Comparison of the XRD patterns of polyaniline samples prepared with acid-to-aniline ratios of 10 and 100 (Fig. 13) reveals six peaks at $2\theta = 6.1$, 8.2, 12.5, 17.4, 21.24, and 25.12 for the polyaniline with the higher acid-to-aniline molar ratio and four peaks at $2\theta = 6$, 8, 11.5, 19.8, and 23.02 for the polyaniline with the lower acid-to-aniline molar ratio.

For the sample with the acid-to-aniline molar ratio of 100, the peak at $2\theta = 25.12$ may be ascribed to periodicity perpendicular to the polymer chain whereas the peak at $2\theta = 21.24$ can be assigned to periodicity parallel to the polymer chain [38]. A shift toward lower diffraction angles is observed for the sample prepared using the lower acid-to-aniline molar ratio. This is because of the effect of the acid-to-aniline molar ratio used during synthesis on the crystallinity of the polyaniline product. It has been reported that increasing the acid-to-aniline molar ratio increases the degree of crystallinity of the product [39]. The increase in

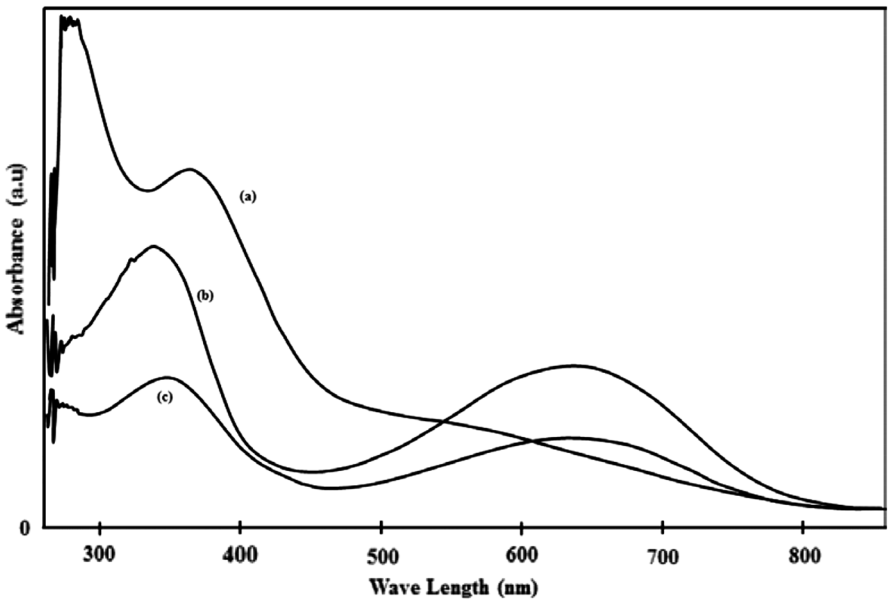

Fig. 12 UV-Visible spectra of the samples synthesized at the same acid/aniline molar ratio with different acid molar concentrations: 0.1 M (**a**), 0.5 M (**b**), and 1 M (**c**)

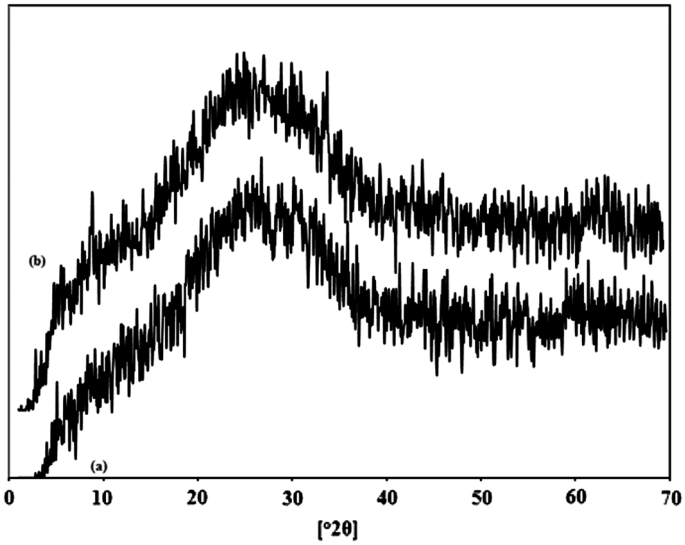

Fig. 13 XRD patterns of polyaniline samples with (**a**) acid/aniline = 10 and (**b**) acid/aniline = 100

the degree of crystallinity and crystallite size of polyaniline with increasing acid concentration is because of the presence of excess protons, which increases d-spacing and interchain separation [40]. However, for both samples a peak centered at $2\theta \sim 6$ is observed, which reflects the nanofibrous structure [41].

Conclusions

Highly efficient synthesis of polyaniline nanofibers was readily achieved by rapid mixing of aniline and APS oxidant in an aqueous acidic solution in the absence of mechanical agitation. No hard or soft templates were used in the method. The effects of different synthetic conditions on the size and morphology of the polyaniline product were investigated. The results showed that fiber diameter could be directly controlled by appropriate selection of dopant, monomer, and oxidant concentrations. Moreover, the efficiency of the process is strongly affected by the synthetic conditions. The results confirmed that this method is scalable to produce bulk quantities of high-quality nanofibers.

Acknowledgments The authors are grateful to Dr H. Shariat Panahi and the laboratories of the Coating Research Center of RIPI.

References

1. G. Li, Ch. Zhang, Y. Li, H. Peng, K. Chen, Polymer **51**, 1934–1939 (2010)
2. D. Li, J.X. Huang, R.B. Kaner, Acc. Chem. Res. **42**(1), 135–145 (2009)
3. A. Kalendova, D. Vesely, J. Stejskal, Prog. Org. Coat **62**, 105–116 (2008)
4. S. Sathiyanarayanan, C. Jeyaprabha, G. Venkatachari, Mater. Chem. Phys. **107**, 350–355 (2008)
5. C. Bian, A. Yu, Synth. Met. **160**, 1579–1583 (2010)
6. S. Sivakkumar, J.S. Oh, D.W. Kim, J. Power Sour. **163**, 573–577 (2006)
7. R. Arsat, X.F. Yu, Y.X. Li, W. Wlodarski, K. Kalantar-zadeh, Sens. Actuators B. Chem. **137**, 529–532 (2009)
8. J. Elizalde-Torres, H. Hu, A. Garcia-Valenzuela, Sens. Actuators B. Chem. **98**, 218–226 (2004)
9. J.X. Huang, R.B. Kaner, J. Am. Chem. Soc. **126**, 851–855 (2004)
10. S. Bhadra, D. Khastgir, N.K. Singha, J.H. Lee, Prog. Polym. Sci. **34**, 783–810 (2009)
11. C. Laslau, Z.D. Zujovic, L. Zhang, G.A. Bowmaker, J. Travas-Sejdic, Chem. Mater. **21**, 954–962 (2009)
12. M. Zhao, X. Wu, Ch. Cai, J. Phys. Chem. **113**, 4987–4996 (2009)
13. Q. Sun, Y. Deng, Eur. Polym. J. **44**, 3402–3408 (2008)
14. D. Wang, F. Ma, Sh. Qi, B. Song, Synth. Met. **160**(19–20), 2077–2084 (2010)
15. D. Li, R.B. Kaner, J. Am. Chem. Soc. **128**, 968–975 (2006)
16. E.M. Genies, A. Boyle, M. Lapkowski, C. Tsintavis, Synth. Met. **36**, 139–182 (1990)
17. A.G. MacDiarmid, J.C. Chiang, A.F. Richter, A.J. Epstein, Synth. Met. **18**, 285–290 (1987)
18. J.X. Huang, R.B. Kaner, Angew. Chem. Int. Ed. Engl. **43**, 5817–5821 (2004)
19. J.X. Huang, Pure Appl. Chem. **78**, 15–27 (2006)
20. J.X. Huang, R.B. Kaner, Chem. Commun. **4**, 367–376 (2006)
21. N.R. Chiou, A.J. Epstein, Adv. Mater. **17**, 1679–1683 (2005)
22. H.D. Tran, Y. Wang, J.M. D'Arcy, R.B. Kaner, ACS Nano **2**, 1841–1848 (2008)
23. S.P. Surwade, N. Manohar, S.K. Manohar, Macromolecules **42**, 1792–1795 (2009)
24. L.H.C. Mattoso, A.G. MacDiamid, A.J. Epstein, Synth. Met. **68**, 1–11 (1994)
25. K.G. Neoh, E.T. Kang, Polymer **34**(18), 3921–3928 (1993)
26. S. Bhadra, N.K. Singha, D.J. Khastgir, Appl. Polym. Sci. **104**, 1900–1904 (2007)
27. Y. Wang, M.F. Rubner, Synth. Met. **47**, 255–266 (1992)
28. Q. Tang, J. Wu, X. Sun, Q. Li, J. Lin, Langmuir **25**(9), 5253–5257 (2009)
29. E.T. Kang, K.G. Neoh, K.L. Tan, Prog. Polym. Sci. **23**, 277–324 (1998)
30. J. Tang, X. Jing, B. Wang, F. Wang, Synth. Met. **24**, 231–238 (1988)
31. I. Sedenkova, J. Prokes, M. Trchova, J. Stejskal, Polym. Degrad. Stab. **93**, 428–435 (2008)
32. S. Bhadra, S. Chattopadhyay, N.K. Singha, D. Khastgir, J. Appl. Polym. Sci. **108**, 57–64 (2008)
33. V. Luthra, R. Singh, S.K. Gupta, A. Mansingh, Curr. Appl. Phys. **3**, 219–222 (2003)
34. N.T. Tung, H. Lee, Y. Song, N.D. Nghia, D. Sohn, Synth. Met. **160**, 1303–1306 (2010)

35. A.A. Athawale, M.V. Kulkarni, W. Chabukswar, Mater. Chem. Phys. **73**, 106 (2002)
36. W. Chen, H.T. Lee, Synth. Met. **47**, 233 (1992)
37. P. Chowdhury, B. Saha, J. Appl. Poly Sci. **103**, 1626–1631 (2007)
38. C.F. Zhou, X.S. Du, Z. Liu, S.P. Ringer, Y.W. Mai, Synth. Met. **159**, 1302–1307 (2009)
39. X.S. Du, C.F. Zhou, G.T. Wang, Y.W. Mai, Chem. Mater. **20**, 3806–3808 (2008)
40. S. Bhadra, N.K. Singha, S. Chattopadhyay, D. Khastgir, J. Polym. Sci.: B **45**, 2048–2059 (2007)
41. J. Yin, X. Zhao, X. Xia, L. Xiang, Y. Qiao, Polymer **49**, 4413–4419 (2008)
42. J. Li, X. Tang, H. Li, Y. Yan, Q. Zhang, Synth. Met. **160**, 1153–1158 (2010)